Growth of residual stress-free ZnO films on SiO$_2$/Si substrate at room temperature for MEMS devices

Jitendra Singh, Sapana Ranwa, Jamil Akhtar, and Mahesh Kumar'

Growth of residual stress-free ZnO films on SiO₂/Si substrate at room temperature for MEMS devices

Jitendra Singh,[1] Sapana Ranwa,[2] Jamil Akhtar,[1] and Mahesh Kumar[2,a]

[1]*Sensors & Nanotechnology Group, CSIR-Central Electronics Engineering Research Institute, Pilani, Rajasthan 333031, India*
[2]*Department of Electrical Engineering, Indian Institute of Technology Jodhpur, Jodhpur 342011, India*

ZnO thick Stress relaxed films were deposited by reactive magnetron sputtering on 2"-wafer of SiO₂/Si at room temperature. The residual stress of ZnO films was measured by measuring the curvature of wafer using laser scanning method and found in the range of 0.18×10^9 to 11.28×10^9 dyne/cm² with compressive in nature. Sputter pressure changes the deposition rates, which strongly affects the residual stress and surface morphologies of ZnO films. The crystalline wurtzite structure of ZnO films were confirmed by X-ray diffraction and a shift in (0002) diffraction peak of ZnO towards lower 2θ angle was observed with increasing the compressive stress in the films. The band gap of ZnO films shows a red shift from ~3.275 eV to ~3.23 eV as compressive stress is increased, unlike the stress for III-nitride materials. A relationship between stress and band gap of ZnO was derived and proposed. The stress-free growth of piezoelectric films is very important for functional devices applications. © 2015 Author(s). All article content, except where otherwise noted, is licensed under a Creative Commons Attribution 3.0 Unported License. [http://dx.doi.org/10.1063/1.4922911]

I. INTRODUCTION

ZnO thin films have been extensively studied due to its co-existing semiconducting, optical and piezoelectric properties.[1] Moreover, ZnO is bio-safe, biocompatible[2] and its promising applications in surface acoustic wave, bulk acoustic wave, optical waveguides, filter and sensor devices because of its piezoelectric nature.[3,4] ZnO films also have compatibility with standard silicon fabrication process. For reliable and high performance devices, ZnO films must have good crystal quality, smooth, stress-free and high piezoelectric properties. Stress free high sensitive piezoelectric ZnO films on insulating substrates are always challenge for researchers.[5,6] Physical properties of ZnO thin films deposited by sputtering strongly depends on growth parameters such as sputtering pressure, substrate temperature, power, gas flow rate etc.[7,8] Biaxial stress primarily produced in ZnO thin films due to confined conditions imposed by underlying substrate and deposition parameters. Large residual stresses develop in ZnO thin films due to intrinsic or thermal stress produced by a mismatch between the thermal contractions of the film and the substrate.[9,10] The residual stresses in ZnO films was measured using X-Ray diffraction (XRD) by Conchon *et al.*[11] and found that deposited films are highly compressively stressed.

Stress in ZnO films exhibits poor performance, low reliability and poor yield of the devices when used in practical devices.[12,13] Due to the existence of high residual stress in ZnO films, a curvature in the wafer were mostly observed and results buckling in the films.[14] This buckling leads to cracks formation and results to poor performance and reliability. Therefore, stress free piezoelectric films are essential requirement for practical and reliable micro-electro-mechanical-system (MEMS) based acoustic devices.[15–17]

---

[a]Corresponding author E-mail address: mkumar@iitj.ac.in

Stress free ZnO thin film can be deposited via using unique sputtering deposition conditions.[18,19] Jou *et al.*[20] optimized sputtering pressure which is 17 mTorr for 1:1 Ar, oxygen ratio for stress free ZnO thin film deposition. However, residual stress also effect the optical properties of ZnO thin films.[9,10,21,22] The Band gap of ZnO films shows red/blue shift with increasing compressive/tensile biaxial stress, unlike the stress in GaN films but both semiconductor shows same behaviour for change in lattice constant (c). Li *et al.*[23] measured tensile stress in ZnO films deposited on quartz by X-ray diffraction technique and a blue shift was observed in optical band gap with increasing tensile stress. The minimum stress was found to be ~14.5 x 10^9 dynes/cm^2. Mohanty *et al.*[24] studied thickness dependent stress in ZnO thin films on glass and found a compressive stress of ~8.4 x 10^{10} dynes/cm^2 in 84 nm thin film. Kumar *et al.*[9] measured a red shift in band gap with increasing tensile stress in GaN layers on Si and linear relationship was derived between stress and band gap. It is also important to study change in lattice constants with residual stress mainly because of change in cell volume of ZnO or GaN. Ping *et al.*[25] reported that lattice constant(c) increases linearly with compressive stress. Rieger *et al.*[26] reported the influence of biaxial compressive stress on optical bandgap and lattice constant of GaN thin film on sapphire with thickness variation of AlN buffer layer .With increasing biaxial compressive stress, band gap (blue shift) as well as lattice constant(c) also increases. MEMS based piezoelectric devices must be processed in the range of room temperature to 150°C for functional layer (ZnO, AlN, PZT etc.) deposition because of inter-diffusion among metal and oxide layers at higher temperature.[7] To overcome this problem a process should be established at room temperature. In the present work, we have deposited thick ZnO films on SiO$_2$/Si wafers at room temperature and study the stress effects on optical properties.

II. EXPERIMENTAL PROCEDURE

ZnO films were deposited by reactive magnetron sputtering using 6" diameter high purity Zn (99.999%) metallic target. Si (100) 2-inch wafers of p-type was boiled in organic solvents trichloroethylene, acetone and methanol, respectively and followed by deionized water (DI). Further, organic residues removed in piranha (H$_2$SO$_4$:H$_2$O$_2$ = 5:1) solution. Native oxide removed in 5% HF solution and then rinsed with DI water. Dried wafer loaded in chamber for 1μm silicon oxide (SiO$_2$) deposition. The SiO$_2$ layers work as an isolation layer between underlying Si substrate and ZnO film. The SiO$_2$ layer thickness and RMS roughness are 1.02 μm and 2-3 nm measured by spectroscopic ellipsometry method and AFM, respectively. The base vacuum of sputtering chamber was achieved around ~2×10^{-6} Torr. Sputter pressure was varied from 10 to 50 mTorr and a set of five samples were prepared. The thickness of ZnO films was kept around ~1μm in all the samples. Film deposition rate was monitored by Inficon digital thickness monitor. The ratio of Ar:O$_2$ =2:3 was maintained during the deposition. RF power and target-substrate distance were kept 450 W and 11 cm, respectively. Stress was mapped by using dual laser switching technology using Film Stress Measurement (FSM) tool. Stress mapping of the wafer were carried out using un-deposited and deposited ZnO wafers. Crystalline structure and surface morphology of ZnO thin film were investigated by Bruker X-ray diffractometer (XRD) and atomic force microscopy (AFM). To measure the optical band gap, ZnO films were deposited on SiO$_2$/glass and transmittance spectra of ZnO films were recorded using high sensitivity 3600 UV-Vis-NIR Spectrophotometer (wavelength range 200-1100nm).

III. RESULTS AND DISCUSSION

In-plane stress in ZnO thin films was measured by using dual laser switching technology using Film stress Measurement (FSM) tool which based on Stoney's equations. Initially, bare wafer of SiO$_2$/Si was laser scanned and curvature was measured. Consequently, ZnO films were deposited by varying sputter pressure in the 10-50 mTorr range. The ZnO film thickness was maintained ~1μm in all the cases, to rule out the effect of film thickness on measured stress. Further, same wafer was again mapped and measured stress profiles are shown in Fig. 1. It is clearly noted that, there is change in wafer curvature due to ZnO layer deposition. Moreover, this indicates that the presence of
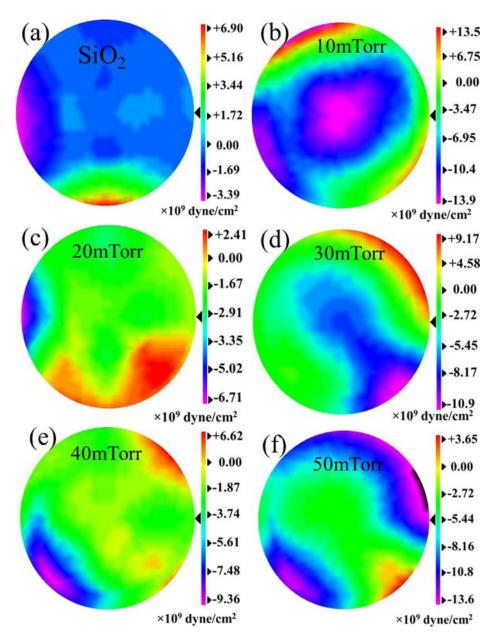
FIG. 1. (a) Stress mapping profile of SiO$_2$/Si wafer and (b)-(f) ZnO film on 2-inch diameter SiO$_2$/SO wafers, samples are prepared in 10-50mTorr range.

compressive stress in ZnO film. Film stress (σ_f) is given by Stoney's equation[27]

$$\sigma_f = \frac{E_s D_s^2}{6(1 - v_s)} \cdot \frac{1}{d_f} \cdot \frac{1}{R} \tag{1}$$

The subscripts f and s denotes thin film and substrate respectively. E and v are Young's modulus and Poisson's ratio respectively. D_s is the substrate thickness whereas d_f is the film thickness. The stress is measured by wafer curvature method and this facilitates us to measure direct stress mapping profile compared to other stress measurement method. Stress was found in the -1.8×10^8 to -11.28×10^9 dyne/cm^2 and compressive in nature.

Fig.2 shows the X-ray diffraction 2θ-ω scan of ZnO film deposited at 10 to 50 mTorr sputter pressures. In diffraction pattern only strong peak corresponding to ZnO (0002) was observed,
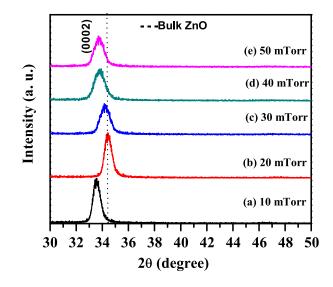
FIG. 2. X-ray diffraction 2θ-ω scan of ZnO film deposited at (a) 10, (b) 20, (c) 30, (d) 40 and (e) 50 mTorr sputter pressure. Dotted line indicates the position of Bulk ZnO.

which indicates that ZnO films are highly c-axis oriented and having wurtzite crystal structure.[28] The surface free energy is minimal in wurtzite structure and ZnO film was grow in c-axis direction.[1] The full width half maxima (FWHM) of diffraction peak increases with sputter pressure which indicates that ZnO crystal quality degraded with increase in sputter pressure. The XRD peak position strongly depends on processing parameters and pattern shows that the diffraction peak (0002) shifted towards lower 2θ angle with respect to bulk 2θ = 34.42° value.[23] The deviation in 2θ values shows ordered behavior with sputter pressure. For 10 mTorr deposited films 2θ = 33.62° , indicates that grown film is under large compressive stress due to unit cell distortion. The ZnO film deposited at 10 mTorr shows much higher value (~5.327 Å) of lattice parameter c compared to bulk value (5.20 Å). As a result, ratio of c/a ~1.6 for wurtzite phase is no longer maintained and elongated along c-axis direction.[23,24] As a consequence, the lattice parameter in basal plane is compressed to maintain unit cell volume constant. This distortion in the unit cell results to higher compressive stress (-11.28×10^9 dyne/cm^2) in the sample deposited at 10 mTorr probably due to extensive bombardment of energetic particles on film surface. The negative sign of stress indicate that lattice constant c of deposited films elongated along the growth direction. The reactive sputter deposition may induce native defects and interstitial sites in growing film due to extensive bombardment at higher RF power (450W). The elongation of unit cell in c-axis direction and thereby giving distortion in unit cell leads to compressive stress. Further, at higher sputter pressure (50mTorr) collision between energetic species are very high and mean free path is decreased. This may also restrict the incorporation of appropriate oxygen content in ZnO crystalline growth. At higher sputter pressure (50mTorr) deposition rate is ~0.5Å/sec which is lower than 10mTorr (1.4Å/sec) deposited films. The adatom surface mobility is reported to be less at higher sputter rate. ZnO film grown at 20 mTorr shows the peak position (0002) at 2θ = 34.42° corresponding to bulk value and lattice is relaxed (-1.8×10^8 dyne/cm^2). Thus, the growth thermodynamics and deposition parameters play a key role for stress relaxed and c-axis orientation ZnO films.

For hexagonal structure, the lattice constant (c) can be calculating using[10]

$$\frac{1}{d^2} = \frac{4}{3}\left(\frac{(h^2 + hk + k^2)}{a^2}\right) + \frac{l^2}{c^2} \qquad (2)$$

Where h, k, l are miller indices and a, b, c are lattice parameter along x, y, z axis, respectively. For (0002) plane and using braggs law ($n\lambda = 2d \sin\theta$), lattice constant (c) can be directly calculating using
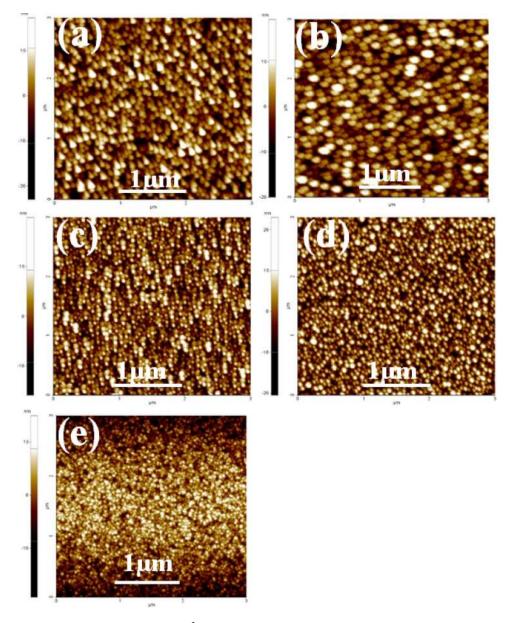
FIG. 3. (a)-(e) show AFM images (3 x 3 μm²) of deposited ZnO films in the range of 10 to 50mTorr sputter pressure, respectively.

$$c = \frac{\lambda}{\sin\theta} \tag{3}$$

Surface morphologies were investigated by using AFM and shown in Fig. 3. It clearly indicates that films are very smooth and having low surface roughness. As sputtering pressure varies from 10 to 50 m Torr, root mean square (RMS) roughness decreases from 5.33 nm to 4.40 nm. Fig. 4(a)-4(b) show relationship between RMS roughness, growth rates and sputter pressure. Further, it is noted that relatively higher surface roughness (∼5.33 nm) obtained for 10 mTorr deposited films, due to high growth rate of deposition at low pressure. For low deposition pressure, deposited atom does not get sufficient time to settle down on substrate and increases film roughness. The growth rates are decreased with increasing sputter pressure due to decreased mean-free path of sputtered atoms. The surface roughness is slightly decreases with pressure but XRD FWHM increases, which reduce the crystalline quality of ZnO.
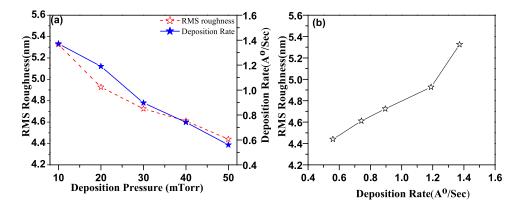
FIG. 4. (a) RMS roughness and growth rate versus Sputter pressure and (b) RMS roughness versus sputter pressure.

Compressive stress commonly exists in ZnO film due to the constraints imposed by underlying substrate and processing conditions. However, stress is undesirable for practical applications of ZnO films. Lattice mismatch and thermal expansion coefficient difference of film and substrate produces extrinsic stress in thin films.[29,30] In present case, thermal expansion coefficient of ZnO film (α_{ZnO} = 2.9 x 10^{-6} K^{-1}) and SiO$_2$ substrate (α_{SiO2} = 0.6 x 10^{-6} K^{-1}) and films were deposited at room temperature. The average stress, 2θ peak position, FWHM, band gap and RMS roughness of ZnO films are listed in Table I. The minimum stress was observed for 20 mTorr deposited films. ZnO films deposited at 10 mTorr partial pressure were found under large compressive stress, which indicates the unit cell elongation along *c*-axis direction and compression in basal plane. Effectively, at lower sputter pressure, mean free path of species is higher. At lower deposition pressure, film deposition rate is relatively higher and depositing species has a less scattering with gas molecules. Nearly stress free films were deposited at the 20 mTorr with a unique combination of processing parameters.

Residual stress significantly affects the band gap of thin films.[31] Consequently, shift in band gap can be correlated with in-plane stress. ZnO thin films were deposited on SiO$_2$ coated glass substrate at same deposition parameters and UV-Visible transmittance spectra were recorded at room temperature. Fig. 5(a) shows the transmittance spectra of 10-50 mTorr range deposited ZnO films. The result shows that nearly all films have transmittance better than 75%. The sputter pressure influences the optical properties of depositing films. The estimated band gap of ZnO films as a function of growth pressure is shown in Fig. 5(b). It may be noted that fundamental absorption edge of ZnO film was found to show red shift with increase in compressive stress. The band gap of ZnO films was estimated by extending linear region of $(\alpha h\nu)^2$ versus $h\nu$ curve, where α is considered as absorption coefficient. The ZnO film thickness (*d*) and transmittance (*T*) are experimentally known parameters. Hence, absorption coefficient $\alpha = (1/d)\ln(1/T)$ calculated. The stress is mainly responsible for red shift in band gap (E$_g$). The in-plane stress (σ_f) can be directly correlated with bang gap (E$_g$) using follows relation by using linear fitting equation:

$$E_g = 3.277 - 0.0041\sigma_f \qquad (4)$$

TABLE I. Measured and estimated ZnO thin film parameters.

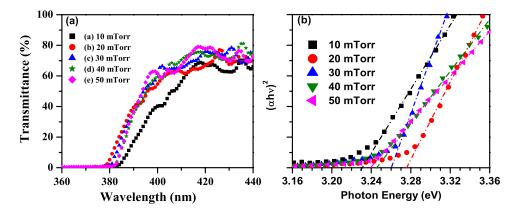| Sample ID	Stress x10^9 (dyne/cm^2)	2θ (degree)	FWHM (degree)	Band gap (E$_g$)	RMS values (nm)	Sputter pressure (mTorr)
Z2	−0.18	34.42	0.69	3.275	4.93	20
Z3	−5.07	34.21	0.92	3.26	4.73	30
Z4	−8.23	33.80	0.87	3.245	4.61	40
Z5	−8.39	33.74	0.91	3.24	4.40	50
Z1	−11.28	33.62	0.68	3.23	5.33	10

FIG. 5. (a) Transmittance spectra of ZnO films deposited from10 to 50mTorr sputter pressure, (b) absorption coefficient plotted with photon energy for band gap estimation.

Where optical band gap of stress free ZnO film is 3.277 eV, which is comparable to bulk ZnO band gap. This fitting curve indicates that optical band gap E_g (eV) has its linear relation with in-plane stress σ_f (dyne/cm^2). Further, it is noted that and band gap decreases with increase in compressive stress. ZnO film bandgap (E$_g$) plotted with in-plane compressive stress and liner fitting data are shown in Fig. 6(a). The negative sign of σ_f indicated that grown film is under compressive stress.[32] As discussed, there are many sources of stress in ZnO films such as lattice mismatch, thermal expansion coefficient mismatch, thickness and processing parameters.[33] Here, the measured compressive strain is mainly caused by sputter pressure. This lattice distortion with sputter pressure is clearly evidence in XRD pattern and supported by FSM measurement. It is clearly noticed that 10 mTorr deposited film are under large compressive (-11.28×10^9 dyne/cm^2) stress while 20 mTorr deposited films have minimal stress. Furthermore, higher spotter pressure due to higher growth rate at lower sputter pressure ($\geq$20 mTorr) deposited films shows again compressive stress. In fact, stress has its origin in the lattice parameter and lattice parameter changes with deposition conditions. It is well known that optical band gap and lattice constant are highly influenced by biaxial stress for ZnO and GaN. Relationship between stress and optical band gap revelled that compressive stress gives red shift in bandgap for ZnO (blue shift in band gap for GaN) and vice versa.[6,34] Fig. 6(b) shows linear relationship between lattice constant and residual compressive stress. As compressive stress increases, lattice constant (*c*) increases from 5.208 A$^\circ$ to 5.327 A$^\circ$ Mathew *et al.*[35] calculated stress induced by ZnO thin film on glass shows tensile in nature and it shows blue shift of optical bandgap (bandgap increases) as well as decreasing lattice constant (c) when tensile stress increases with annealing temperature. In the present case, a red shift was observed in bandgap with increasing compressive stress and lattice constant (*c*) increases with compressive stress.
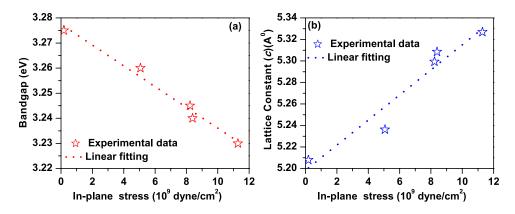

FIG. 6. (a) Bandgap (E$_g$) versus in-plane compressive stress of ZnO films, and (b) Lattice constant (*c*) variation with in-plane compressive stress.

IV. CONCLUSION

Stress relaxed highly c-axis oriented ZnO films are deposited at room temperature by reactive sputtering technique. Compressive stress in ZnO films is highly dependent on sputter pressure and gives stress free ZnO film at 20 mTorr pressure. XRD (0002) peak shifts from 34.42º to 33.62º as residual compressive stress increased from 0.18×10^9 to 11.28×10^9 dyne/cm^2. A red shift was observed in optical band gap with increasing compressive stress and band gap decreased from 3.275eV to 3.23 eV with increases in compressive stress from -0.18×10^9 dyne/cm^2 to -11.28×10^9 dyne/cm^2. Linear relationship has been proposed between stress and band gap which shows optical band gap of stress free ZnO film is 3.27 eV. Lattice constant (*c*) also increases from 5.20 to 5.32 A$^\circ$ as in-plane compressive stress increases from -0.18×10^9 dyne/cm^2 to -11.28×10^9 dyne/cm^2 because the stress produces elongation of *a, b* lattice parameters. The stress relaxed piezoelectric ZnO films are very important for practical devices applications.

[1] U. Ozgur, Y. I. Alivov, C. Liu, A. Teke, M. A. Reshchikov, S. Dogan, V. Avrutin, S. J. Cho, and H. Morkoç, J. Appl. Phys. **98**, 041301 (2005).
[2] Z. L. Wang and J. Song, Science **312**, 242 (2006).
[3] R. Baraki, N. Novak, T. Frömling, T. Granzow, and J. Rödel, App. Phys. Lett. **105**, 111604 (2014).
[4] Y.Q. Fu, J.K. Luo, X.Y. Du, A.J. Flewitt, Y. Li, G.H. Markx, A.J. Walton, and W.I. Milne, Sensors and Actuators B **143**, 606 (2010).
[5] J. G. E. Gardeniers, Z.M. Rittersma, and G.J. Burger, J. Appl. Phys. **83**, 7844 (1998).
[6] R. Menon, K. Sreenivas, and V. Gupta, J. Appl. Phys. **103**, 094903 (2008).
[7] R. Singh, M. Kumar, and S. Chandra, J. Mater. Sci. **42**, 4675 (2007).
[8] R. Ondo-Ndong, G. Ferblantier, M. A. Kalfioui, A. Boyer, and A. Foucaran, J. Cryst. Growth **255**, 130 (2003).
[9] M. Kumar, B. Roul, T. N. Bhat, M. K. Rajpalke, P. Misra, L.M. Kukrej, N. Singh, A.T. Kalghatgi, and S. B. Krupanidhi, Mat. Res. Bull. **45**, 1581 (2010).
[10] T. P. Rao, M.C. S. Kumar, S. A. Angayarkanni, and M. Ashok, J. Alloy and Comp. **485**, 413 (2009).
[11] F. Conchon, P.O. Renault, P. Goudeau, E. Le Bourhis, E. Sondergard, E. Barthel, S. Grachev, E. Gouardes, V. Rondeau, R. Gy, R. Lazzari, J. Jupille, and N. Brun, Thin Sol. Films **518**, 5237 (2010).
[12] H. J. Trodahla, F. Martin, P. Muralt, and N. Setter, Appl. Phys. Lett. **89**, 061905 (2006).
[13] D. G. Zhao, S. J. Xu, M. H. Xie, and S. Y. Tong, Appl. Phys. Lett. **83**, 677 (2003).
[14] V. Bhatt, S. Chandra, S. Kumar, C. M. S. Rauthan, and P. N. dixit, Indian J. Pure & Appl. Phys. **45**, 377 (2007).
[15] E. Iborra, J. Olivares, M. Clement, J. Vergara, A. Sanz-Hervas, and J. Sangrador, Sens. Actuators, A **115**, 501 (2004).
[16] F. Engelmark, G. Fucntes, I. V. katardjiev, A. Harsta, U. Smithand, and S. Berg, J. Vac. Sci. Technol., A **18**, 1609 (2000).
[17] H. P. Loebl, M. Klee, C. Metzmacher, W. Brand, R. Milsom, and P. Lok, Mat. Chem. Phys. **79**, 143 (2003).
[18] S.B. Krupanidhi and M. sayer, J. Appl. Phys. **56**, 3308 (1984).
[19] R. J. Drese and M. Wuttig, J. Appl. Phys. **98**, 073514 (2005).
[20] J. H. Jou, M.-Y. Han, and D.-J. Cheng, J. Appl. Phys. **71**, 4333 (1992).
[21] R. Ghosh, D. Basak, and S. Fujihara, J. Appl. Phys. **96**, 2689 (2004).
[22] W. Shan, R. J. Hauenstein, A. J. Fischer, J. J. Song, W. G. Perry, M. D. Bremser, R. F. Davis, and B. Goldenberg, Phys. Rev. B **54**, 13460 (1996).
[23] Y. F. Li, B. Yao, Y. M. Lu, C. X. Cong, Z. Z. Zhang, Y. Q. Gai, C. J. Zheng, B. H. Li, Z. P. Wei, D. Z. Shen, X. W. Fan, L. Xiao, S. C. Xu, and Y. Liu, Appl. Phys. Lett. **91**, 021915 (2007).
[24] B. C. Mohanty, Y.H. Jo, D. H. Yeon, I. J. Choi, and Y. S. Choa, Appl. Phys. Lett. **95**, 062103 (2009).
[25] Y. Ping, L. Pei, Z. Li-Qiang, W. Xiao-Liang, W. Huan, S. Xi-Fu, and X. Fang-Wei, Chi. Phys. B **21**, 016803 (2012).
[26] W. Rieger, T. Metzger, H. Angerer, R. Dimitrov, O. Ambacher, and M. Stutzmann, Appl.Phys. Lett. **68**, 970 (1996).
[27] G.G. Stoney, Proc. R. Soc. London, Ser. A. **82**, 172 (1909).
[28] S. Ranwa, P. K. Kulriya, V. Dixit, and M. Kumar, J. Appl. Phys. **115**, 233706 (2014).
[29] M.F. Malek, M.H. Mamat, M.Z. Musa, Z. Khusaimi, M.Z. Sahdan, A.B. Suriani, A. Ishak, I. Saurdi, S.A. Rahmanand, and M. Rusop, J. Alloy. Compd. **610**, 575 (2014).
[30] R. K. Sendi and S. Mahmud, J. Phys. Sci. **24**, 1 (2013).
[31] V. Gupta and A. Mansingh, J. Appl. Phys. **80**, 1063 (1996).
[32] S.Y. Ma, X.H. Yang, X.L. Huang, A.M. Sun, H.S. Song, and H.B. Zhu, J. Alloys. Compd. **566**, 9 (2013).
[33] T. Kim, J. Korean Phys. Soc. **58**, 787 (2011).
[34] S. C. Hsu, B. J. Pong, W. H. Li, T. E. Beechem III, S. Graham, and C. Y. Liu, Appl. Phys. Lett. **91**, 251114 (2007).
[35] J. P. Mathew, G. Varghese, and J. Mathew, Chin. Phys. B **21**, 078104 (2012).